ELSEVIER

Fabrication of sustainable insulation refractory: Utilization of different wastes

SK.S. Hossain*, P.K. Roy

Department of Ceramic Engineering, IIT (BHU), Varanasi 221005, U.P., India

ABSTRACT

The main objective of this study is to evaluate the use of different wastes as a raw material in the fabrication of insulation refractory. These wastes are fly ash, rice husk (RH), rice husk ash (RHA) and fired refractory grog. Various samples are prepared with different compositions based upon partial and fully replacement of clay by FA. Rice husk is used as an additive to produce the pores in the matrix. The specimens are prepared by semi dry process and sintering is performed at 800–1000 °C in air atmosphere. Numerous physical, mechanical and thermal characterizations like apparent porosity (AP), bulk density (BD), cold crushing strength (CCS), linear shrinkages, X-ray diffraction (XRD), scanning electron microscope (SEM) and thermal conductivity measurements of fired samples are done. The results show that the use of waste materials decreases the thermal conductivity and bulk density of the insulation refractory. Cold crushing strength of the 100 wt.% waste materials sample is around 15 MPa. This promising characteristic suggests that these wastes materials may lead to be used as a potential material for the preparation of insulation refractories. The use of waste materials may be economically attractive and technically feasible.

© 2018 SECV. Published by Elsevier España, S.L.U. This is an open access article under the CC BY-NC-ND license (http://creativecommons.org/licenses/by-nc-nd/4.0/).

Fabricación de aislantes refractarios sostenibles: utilización de diferentes residuos

RESUMEN

El objetivo principal de este artículo es evaluar el uso de diferentes residuos como materia prima en la fabricación de aislantes refractarios. Estos desechos son cenizas volátiles, cascarilla de arroz (*rice husk* [RH]), cenizas de cascarilla de arroz (*rice husk ash* [RHA]) y grog refractario cocido. Se prepararon varias muestras con diferentes composiciones basadas en la sustitución parcial y total de arcilla por cenizas volátiles. La cascarilla de arroz se usó como un aditivo para producir poros en la matriz. Las muestras se prepararon mediante un proceso semiseco y la sinterización se realizó a una temperatura de 800 a 1.000 °C en atmósfera de aire. Se realizaron numerosas caracterizaciones físicas, mecánicas y térmicas, como porosidad aparente (*apparent porosity* [AP]), densidad aparente (*bulk density* [BD]), resistencia al aplastamiento en frío (*cold crushing strength* [CCS]), contracciones lineales, difracción de rayos X (*X-ray diffraction* [XRD]), microscopio electrónico de barrido (*scanning electron microscope* [SEM]) y mediciones de conductividad térmica de las muestras cocidas. Los resultados

* Corresponding author.
 E-mail address: skshossain.rs.cer17@iitbhu.ac.in (SK.S. Hossain).

muestran que el uso de materiales de desecho reduce la conductividad térmica y la densidad aparente del aislante refractario. La resistencia al aplastamiento en frío de la muestra de materiales de desecho al 100% en peso es de unos 15 MPa. Esta prometedora característica sugiere que estos materiales de desecho podrían utilizarse como material potencial para la preparación de aislantes refractarios. El uso de materiales de desecho puede ser económicamente atractivo y técnicamente factible.

Introduction

Presently, energy conservation is one of the most vital points for the industry. Therefore, the improvement of the thermal efficiency of industrial furnaces used in the ferrous and non-ferrous industries is becoming essential. The energy losses through furnaces can be effectively reduced by high performance thermal insulation materials used for lining the inside of furnaces [1]. This increases the use of insulating and low thermal conductivity materials. On the other hand, new demand of industries is to utilize the industrial waste materials into commercial products. The benefits are saving energy, saving natural resources and reducing waste disposal. Engaged in this thought, use of wastes, will be a way of sinking the cost of ceramics products. A wide variety of waste materials have been studied for production of insulation bricks such as paper processing residues [2,3], sludge [4–6], petroleum coal dust [7], coal ash [8], rice husk ash [9,10], beverage industry [11,12], olive [13,14] and wheat [15] have been widely investigated. However, to the best of our knowledge, no such investigation for insulation ceramic materials produced with combination of ingredients are fly ash (FA), RHA, RH, refractory grog and clay.

Continue rise in energy demand in emerging countries causes higher usage of coal in thermal power plants. This coal burning by-product is recognized as fly ash, which pollutes the environment and damage cultivated land. Production of FA depends on the various inorganic and organic constituents of the coal [16]. In India coal is of low grade having high ash content around 30–45 wt.%, fly ash produced at coal thermal power stations. Worldwide production of FA is approximately 776MT per-annum whereas India's annual production is estimated around 169MT [17]. This huge amount of FA, if not utilized in right quantity, it will be hazardous to environment. Therefore, it is needed of making alternative technology in order to reduce its possible environmental impacts. FA is a silico-aluminium or low calcium material that makes it suitable to use as a source of geo-polymerization reaction [18,19].

Due to these properties FA gives excellent mechanical strength and good resistance to fire and acid attack. This statistic leads to encourage the researchers to find different applications of FA. Several authors have studied the utilization of FA in different fields for examples of the glass-ceramics [20], inorganic foams [21], zeolites [22], silicon carbides [23], paving blocks [24], tiles [25] and mullite [26].

One of the largest produced crop in the world is rice. Rice husk (RH) is the surface cover of rice grain, which has two interlocking halves. During rice processing around 20% of the rice paddy produces RH in the rice mills [27]. Dumping of RH is an important issue in those countries that cultivate large amounts of rice because it takes very long time to decompose [28]. Normally, RH contains 70–85% organic substance such as cellulose, lignin, etc. and rest inorganic components such as silica, alkalis and trace elements [29,30]. Generally, RH is used as a fuel in the boilers for producing energy through direct combustion or by gasification. These causes further environmental pollution as well as disposal problem when it is burnt, ∼20% of its weight is converted into ash is called rice husk ash (RHA). Characteristics of RHA depend on environmental circumstances of its origin as well as the route acquired during burning conditions of the husk [31]. It contains 80–97% of amorphous silica and this silica shows better reactivity than crystalline silica present in quartz [32]. Different studies are performed in order to utilize the RHA silica for preparation of different ceramics i.e. glazes preparation [33], borosilicate [34], cordierite [35], mullite [36], forsterite [37], silicon carbide [38] and refractory bricks [39].

The main objective of the present study was to provide a new route to utilize the fly ash, refractory grog, rice husk ash and rice husk as pore-forming agents in a composition of insulation refractory. The use of these waste materials not only increases the performance but also attractive with respect to environment, sustainability and economy. This technology may be extended for the production of insulation refractory bricks.

Table 1 – Identification and batch composition of samples.				
Samples	Ball clay (wt.%)	Fly ash (wt.%)	RHA (wt.%)	Grog (wt.%)	RH (wt.%)
s-1	50	0	30	15	5
s-2	40	10	30	15	5
s-3	30	20	30	15	5
s-4	20	30	30	15	5
s-5	10	40	30	15	5
s-6	0	50	30	15	5

Experimental procedure

Pulverized rice husk (RH) and rice husk ash (RHA) were collected from local rice mills, where RH used as a fuel to produce RHA. This RHA contained trace amount of volatile matter as well as carbon. To eliminate this carbon from RHA it was further heated at 600 °C for 2 h and passed through mesh size of 150 μm. FA was collected from "Simhadri Super Thermal Power Plant" (NTPC) situated in Andhra Pradesh, India. It was produced after burning of coal and its properties depended on the composition of coal and efficiency of boiler. FA also heat treated at 700 °C to remove the possibility of any unburnt carbon in the fly ash and sieved to a particle size of ≤90 μm. Fired refractory grogs were collected from refractory industry. The particle size of grogs was ≤350 μm. The ball clay was purchased from Ace Cone Ceramics Ltd., Bikaner, India, contained 52 wt.% SiO_2 and 33 wt.% Al_2O_3.

In this study six different samples were prepared with different compositions containing FA, RHA, RH, refractory grog and ball clay as tabulated in Table 1. In the compositions, clay was replaced by FA, whereas other ingredients were remaining constant. At the very first stage, all ingredients were crushed and passed through the different sizes of sieves i.e. grog (≤350 μm), ball clay (≤90 μm), fly ash (≤90 μm), RHA (≤150 μm), RH (≤75 μm). Then all ingredients were weighed according to batch composition and then mixed by dry milling process for 20 min at 300 rpm in ball mill. After ball milling, least amount of water has been added for semi-dry mixing and the whole mass was mixed for 15 min prior to shaping. Rectangular (40 mm × 10 mm × 2.5 mm) samples were prepared by uniaxial hydraulic press at a pressure of 120 MPa. The pressed samples were dried in an electric air oven at 110 °C for 24 h and then firing were done at different temperature from 800 to 1000 °C for 2 h in air atmosphere with heating and cooling rate of 3 °C/min.

The crystalline phases of ingredients and fired samples were investigated with XRD and data was collected at a scanning rate of 5°/min for 2θ in a range from 10° to 90° with the help of "Rigaku Desktop Miniflex II X-Ray Diffractometer" equipped with Ni filter and Cu Kα radiation (λ) 1.54056 Å (serial no: HD20972, Rigaku Corporation, Tokyo, Japan). The surface morphology of the insulation refractory samples was inspected by scanning electron microscopy (SEM) (ZEISS, EVO 18-2045). Differential thermal and thermogravimetric analysis (DTA–TGA) was carried out for RH in an oxygen atmosphere with a heating rate of 5 °C/min with the help of "KEP Technologies, Setaram Scientific & Industrial Equipment, France (Model-Labsys, serial no-560/51920)". The chemical composition of raw materials was examined by the X-ray fluorescence (XRF) (Philips PW 2400, Netherlands). The apparent porosity (AP) and bulk density (BD) of refractory specimens were estimated by Archimedes method. Total linear shrinkage of fired samples was determined based on the ASTM C356-10 [40]. Cold crushing strength (CCS) and flexural strength were determined according to the method defined in ASTM C133 by Universal Testing Machine, Tinius Olsen, H10KL-I0129 [41]. The thermal conductivity values of the fired samples were measured by hot cross-wire method using thermal conductivity measurement apparatus (VBCC, LOC: 441A102-0005).

Results and discussion

Characterization of raw material

The chemical composition of RHA is presented in Table 2 and found that, heat treated RHA contains greater than 93% of SiO_2. Fig. 1(a) shows the XRD image of heat treated RHA, which indicate that RHA consists of amorphous silica only. This deficiency of long range ordering permits them to react more easily and efficiently with additional surrounding materials. Fig. 2 shows the DTA–TGA curve of pulverized rice husk up to 1000 °C in air atmosphere. Around ~75 wt.% of organic matter of RH was removed when temperature was raised up to 480 °C and no further changes in weight occurs up to 1000 °C, this remaining 25 wt.% material is amorphous silica. So, it can be used as pore forming agent for ceramics because it will
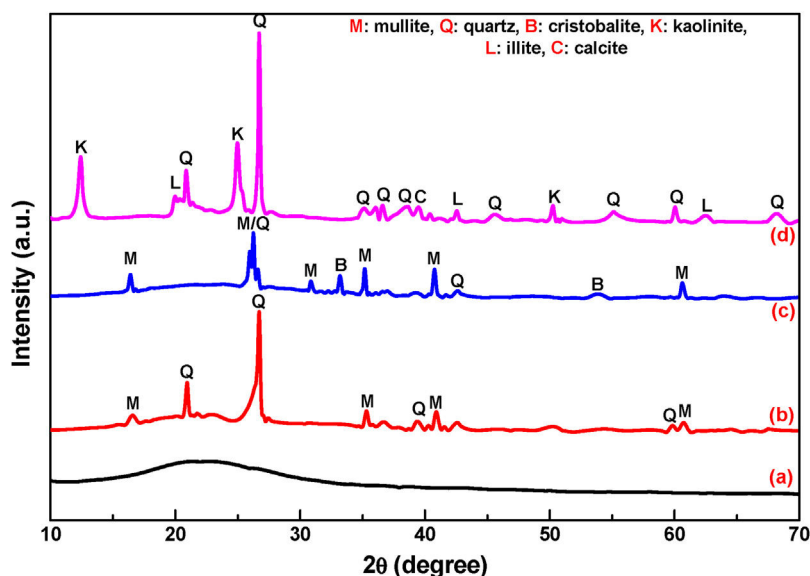

Fig. 1 – XRD curve of (a) heat treated RHA, (b) heat treated fly ash, (c) refractory grog, and (d) ball clay.
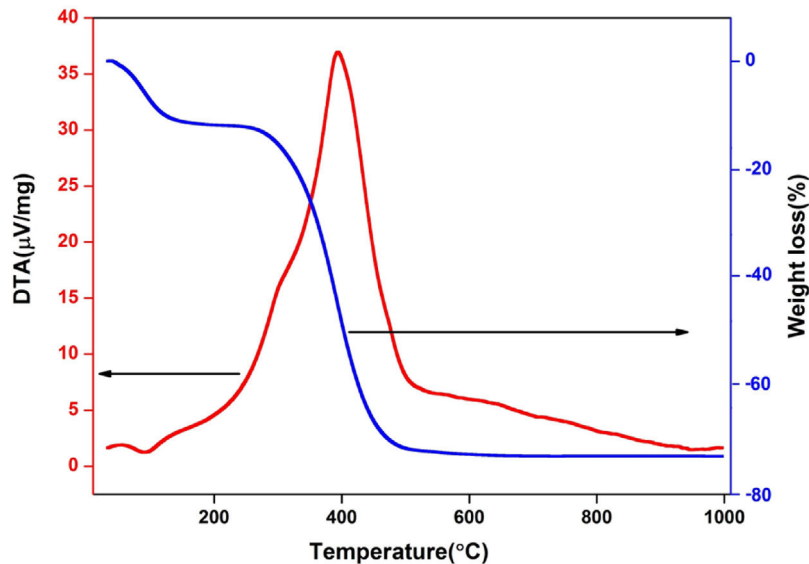
Fig. 2 – DTA–TGA curve of rice husk.

Table 2 – Chemical composition of heat treated fly ash, RHA, ball clay and refractory grog.

Compound (wt.%)	RHA	Fly ash	Grog	Clay
SiO_2	93.28	57.37	62.71	56.14
Al_2O_3	–	29.78	32.17	25.67
CaO	0.53	8.41	–	0.94
Fe_2O_3	0.41	1.83	1.49	2.74
Na_2O	2.75	0.54	1.32	0.63
P_2O_5	1.18	–	–	–
TiO_2	0.21	1.07	0.92	0.35
K_2O	1.22	0.32	0.87	0.78
MgO	0.27	0.68	0.52	0.32
RuO_2	0.15	–	–	–
L.O.I.	–	–	–	12.44

produce pores by combusting itself which is a fundamental requirement of insulating refractory [42].

The chemical composition of FA majorly constituted with silica (SiO_2), alumina (Al_2O_3), calcium oxide (CaO) and ferric oxide (Fe_2O_3). Fig. 1(b) shows the XRD diffraction pattern of heat treated FA, which contains mainly crystalline phase of mullite and quartz. Fig. 3(a) exhibits the particles morphology of the FA; which is shown that the particles are almost

spherical and average size ∼5.28 μm, as estimated from SEM micrograph by software entitled as "Image J1.48V".

The chemical composition of grogs and ball clay are shown in Table 2, which contains silica as a major component. Typical XRD pattern of grogs and clay is shown in Fig. 1(c) and (d), respectively. Grog contains mainly crystalline form of silica and mullite. Consequently, clay contains mainly crystalline phase of quartz, lower amounts of silicates and carbonates. Fig. 3(b) shows the SEM image of ball clay powder, it exhibits irregular-shaped particles with average particle size around ∼7.58 μm.

Characterization of fired insulation brick samples

Porosity of insulating material has a lot of importance with regards to the performance and applications. Insulating properties (thermal conductivity) of bricks depend on the total porosity present in the specimen. The apparent porosity (AP) and bulk density (BD) measurements are done for all sintered samples and mean values are shown in Fig. 4(a) and (b) respectively. It has been observed that incorporating FA by replacing clay in the composition results in significant changes in AP and BD. Apparent porosity increases from 38% to 53% and
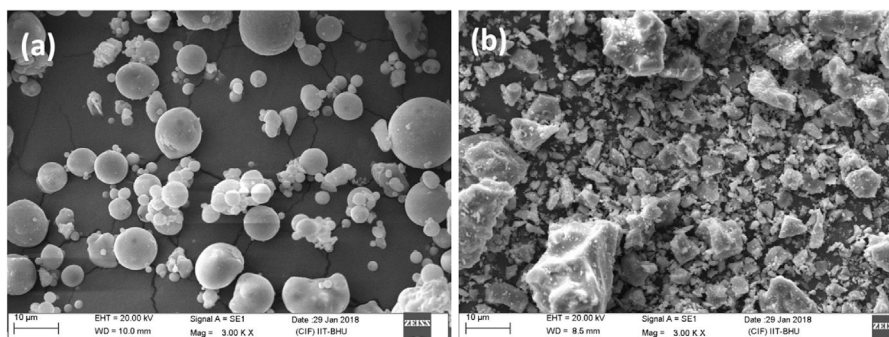

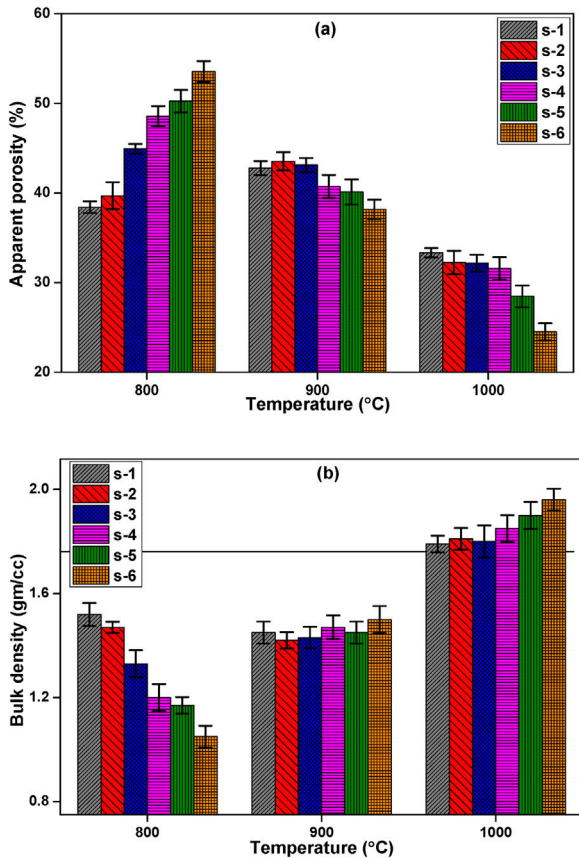**Fig. 3 – SEM images of (a) fly ash and (b) clay.**

Fig. 4 – (a) Apparent porosity and (b) bulk density of fired samples.

bulk density decreases from 1.52 gm/cm^3 to 1.05 gm/cm^3 at 800 °C, similar trends is reported by Otero et al. [43]. RH burns through firing process and forms pores in the structure by releasing CO_2 [44]. When clay is replaced by FA liquid phase decreases, results formed pores cannot be filled completely at 800 °C. As a result densification kinetics is decreases during

low temperature firing at 800 °C. The decrease in density may be due to lower weight of FA then ball clay. When temperature is increased from 800 to 1000 °C, geopolymerisation reaction takes place [19]. RHA contains amorphous silica that is more active, this silica starts diffusion reaction with others grains when increasing the firing temperature than 800 °C [32]. This diffusion of grains and geopolymerisation reaction are eliminates the pores between grains, aid the decreases of porosity and increases in bulk density with increasing temperature.

The typical X-ray diffraction patterns of fired samples are shown in Fig. 5. It is indicated that the samples are mixing of polycrystalline and amorphous broad band. Comparing the XRD patterns, we may observe that the intensity of crystallinity has increased significantly with increasing firing temperature 800 °C–1000 °C. JCPDS data are used to determine the various phases developed after firing i.e. quartz (SiO_2), mullite ($3Al_2O_3·2SiO_2$) and anorthite ($CaO·Al_2O_3·2SiO_2$). However, all samples consist of crystalline silica (SiO_2) as the major phase and with enhancement of FA content in the composition mullite phases intensities are increased.

The change in linear dimension that has happened in the test sample before and after firing is called linear shrinkage or expansion. Table 3 shows the mean values of linear shrinkage for the ceramic samples fired at 800, 900 and 1000 °C along with flexural strength and CCS. It has been seen that the total shrinkage in the all-inclusive refractory samples are quite less i.e. 1.5–5.5%. These results can be imposed to the fired raw materials incorporated in the composition (50–95%) and rice husk addition leads to a decrease in the total linear shrinkage. However, increase of firing temperature causes of enhancement in linear shrinkage of refractory samples. With increasing temperature may be low melting oxides in the clay mineral increase the melted products in the structure causes increase the shrinkage values as well. Based on the results in Table 3, reduction of clay amount in the composition decreases the total linear shrinkage at 800 °C. Significant linear shrinkage is observed when temperature rises at 1000 °C for all samples which may be explained as a result of removal of pores and inter-granular spaces during the firing.
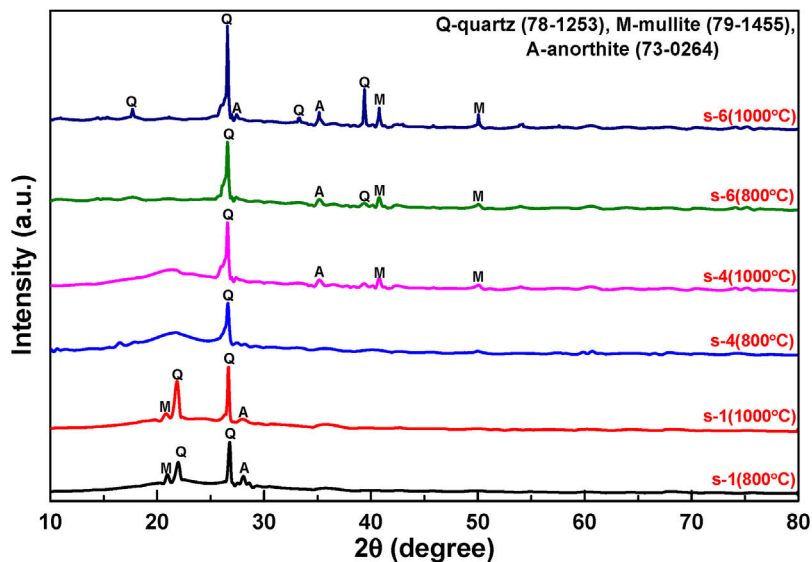

Fig. 5 – XRD analysis of fired samples at 800 and 1000 °C.

Table 3 – Shrinkage, flexural strength and CCS of fired sample at different temperatures.

| Samples	Shrinkage (%)						Flexural strength (MPa)						CCS (MPa)					
	800°C		900°C		1000°C		800°C		900°C		1000°C		800°C		900°C		1000°C	
	Mean	s.d.	Mean	s.d.	Mean	s.d.	Mean	s.d.	Mean	s.d.	Mean	s.d.	Mean	s.d.	Mean	s.d.	Mean	s.d.
s-1	1.90	0.05	2.86	0.08	4.27	0.08	10.28	0.2	8.13	0.3	12.86	0.34	22.56	0.42	19.73	0.24	24.22	0.35
s-2	1.84	0.07	2.61	0.05	4.11	0.09	9.35	0.2	7.46	0.2	13.28	0.19	21.82	0.37	18.96	0.36	24.56	0.24
s-3	1.63	0.04	2.47	0.09	4.02	0.10	8.72	0.25	7.83	0.26	13.89	0.34	18.45	0.28	19.35	0.42	24.80	0.19
s-4	1.56	0.06	2.43	0.07	4.47	0.09	6.02	0.16	9.64	0.34	14.06	0.21	16.83	0.30	20.72	0.37	25.93	0.51
s-5	1.59	0.05	2.35	0.06	4.78	0.08	5.76	0.24	10.12	0.17	15.54	0.27	15.32	0.45	21.46	0.36	27.38	0.45
s-6	1.70	0.07	2.58	0.07	5.02	0.09	4.84	0.27	11.89	0.28	17.11	0.24	14.45	0.24	22.42	0.27	31.54	0.37
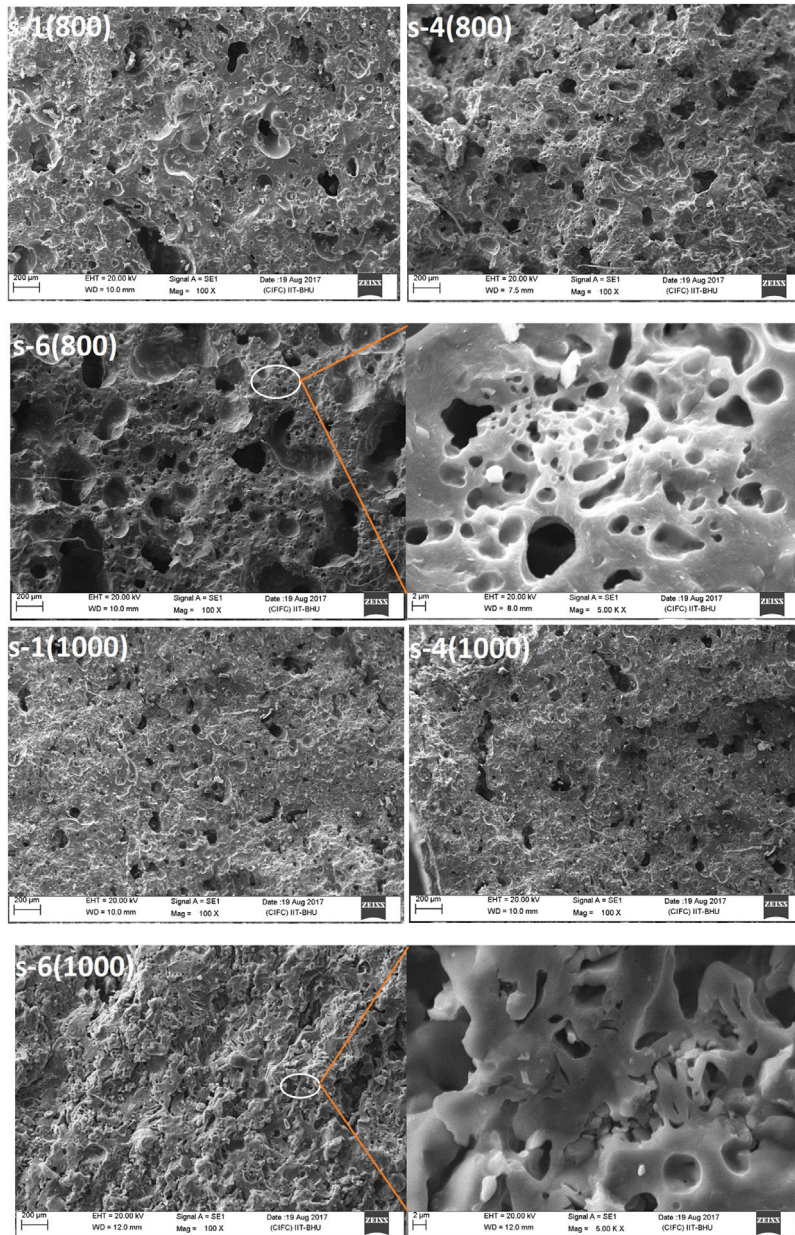
Fig. 6 – SEM image of fired samples.

Fig. 6 exhibits the surface morphology of the fractured cross sectional surface of fired sample. SEM analyses indicate a typical foamy structure with open and close pores at 800 °C. There is no preferential orientation or shape of pores. It is seen that FA content has the mark influences on the pore structure, pore size, and pore distribution of insulation refractory [45].

s-1(800)

Element	Weight %	Atomic %
O K	54.55	68.36
Na K	1.41	1.23
Al K	7.40	5.50
Si K	31.80	22.70
Ca K	3.34	1.67
Fe K	1.50	0.54
Total	100	100

s-6(800)

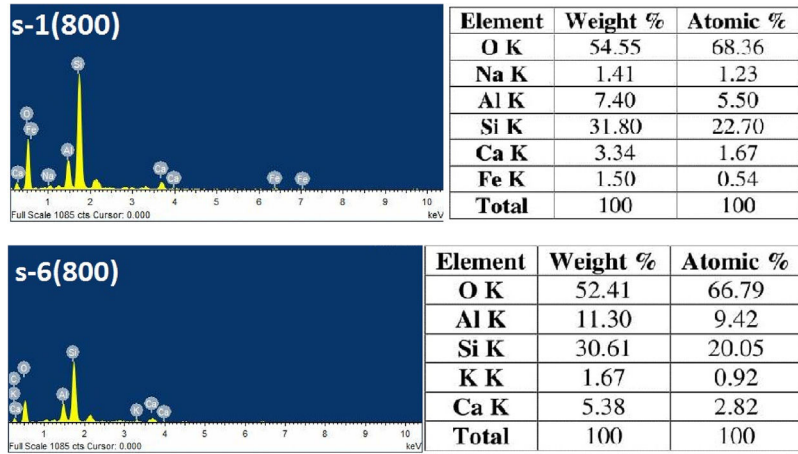| Element	Weight %	Atomic %
O K	52.41	66.79
Al K	11.30	9.42
Si K	30.61	20.05
K K	1.67	0.92
Ca K	5.38	2.82
Total	100	100

Fig. 7 – EDX analysis of fired s-1 and s-6 samples at 800 °C.
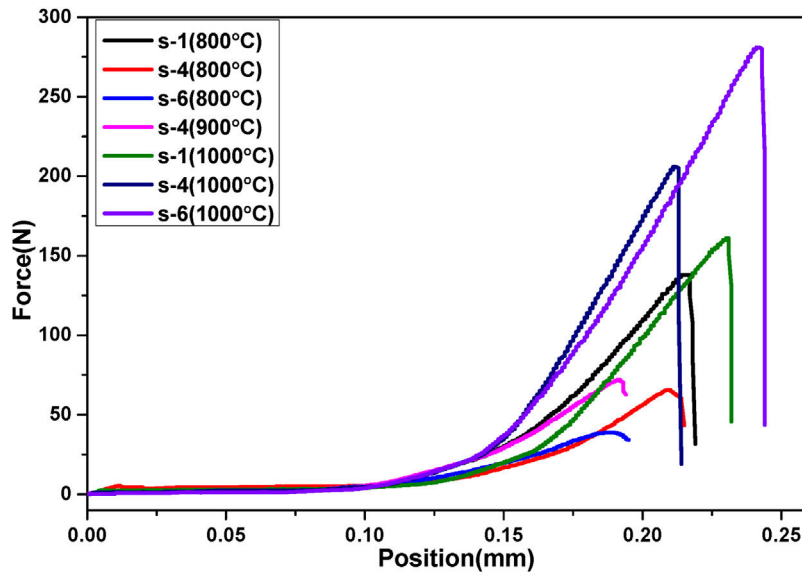

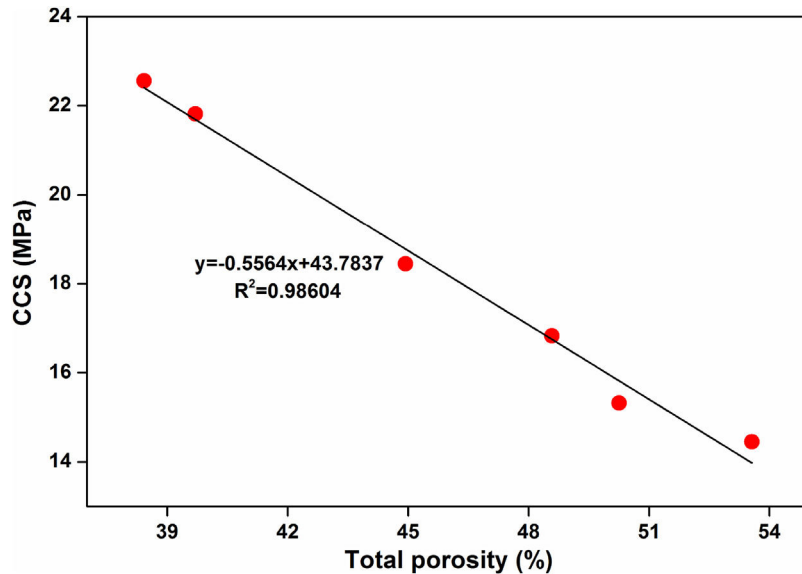Fig. 8 – Bending strength curve of fired sample at 800, 900 and 1000 °C for s-1, s-4 and s-6.

Fig. 9 – Relation between CCS and porosity.

Porous structures are also formed by the burning of RH, which contents ~80% of organic matter. With increasing firing temperature, sintering neck is grown and the pores are shrinking. Accordingly, the pore size is decreased and densification level increases [46]. The EDS analyses are performed to find out the elemental composition of the samples. Fig. 7 show the EDX analysis of 0 and 50 wt.% of FA content sample fired at 800 °C.

Mean values of flexural strength of fired samples is shown in Table 3 and Fig. 8 shows the bending strength curves of some selective fired samples at room temperature. Flexural strength is decreased with increasing ratio of FA in refractory, especially when firing temperature is 800 °C. The values of flexural strength are decreased from 10.28 to 4.84 MPa due to increasing of porosity and pore size as shown in SEM image. Therefore, crack concentration in the non-ductile body is increases; as a result less value of stress is required for breaking [47]. However, strength is increased with temperature due to the higher sintering degree of the samples and the development of crystalline phases by the reaction of FA and RHA silica. As understood from this study waste concentration in the body and firing temperatures of bricks have significant effects on strength of refractory.

Cold crushing strength (CCS) is a very important parameter for insulating bricks. CCS of the samples as shown in Table 3 are measured at room temperature after firing at 800, 900 and 1000 °C for 2 h. It is found that these insulating samples have shown good mechanical strength, these results may be attributed to the presences of fired refractory grogs into the composition. Refractory grogs act as a non-shrinkage material that increasing the stress resists ability of the bricks [39]. Table 3 shows that the CCS of samples is decreased with the increase in fly ash addition. CCS values are decreased to almost 36% for fully replacement of clay with FA when firing at 800 °C. Due to presence of higher percent of open pores may cause the loss of strong bonding in the structure results decrease the CCS of bricks [48]. CCS values of samples are remarkably improved with firing at higher temperature. It has seen that decrease in porosity and increases in bulk density with increasing temperature. As a result, CCS of bricks is increased with increasing firing temperature of insulating refractory. Usually, it is considered that CCS of brick specimens mostly depend on their density, porosity and pores size distributions [49]. A linear relationship was observed between CCS and total porosity for samples fired at 800 °C as shown in Fig. 9.

The thermal conductivity measurement is quite essential for insulation refractories. Many factors like application temperature, chemical and mineralogical compositions, complexity of structure and defect are affecting the thermal conductivity of refractories. Fig. 10(a)–(c) shows the temperature dependence thermal conductivity of fired samples at 800, 900 and 1000 °C respectively, measurement are performed at temperatures 200 °C, 600 °C and 1000 °C. It is seen that the thermal conductivity coefficient of all samples are enhanced with the increasing firing temperature of samples. It may be due to decrease in porosity with increasing firing temperature. Thermal conductivity values of samples decreases with the addition of FA may be due to increase of apparent porosity and decreases of densification. This porosity acts as a fence to the flow of heat and as a result thermal conductivity of samples drop [42]. Fig. 11 shows the relationship of between thermal

conductivity and apparent porosity of fired samples at 800 °C. In sample s-6 the conductivity slightly increases may be the effect of pore size. The effects of radiation on pore conductivity are increased with the increasing pore volume. Pores of large size are increasing the conductivity whereas small pores remain a good barrier to radiation effect with increasing temperature [50]. It is seen that the thermal conductivity values is increased with increasing measurement temperature of conductivity. Heat transfer through a solid happens via energy transfer between vibrating atoms by phonons, photons, electrons, ions, etc. For refractory materials, phonons and photons are the key media for thermal conductivity, and
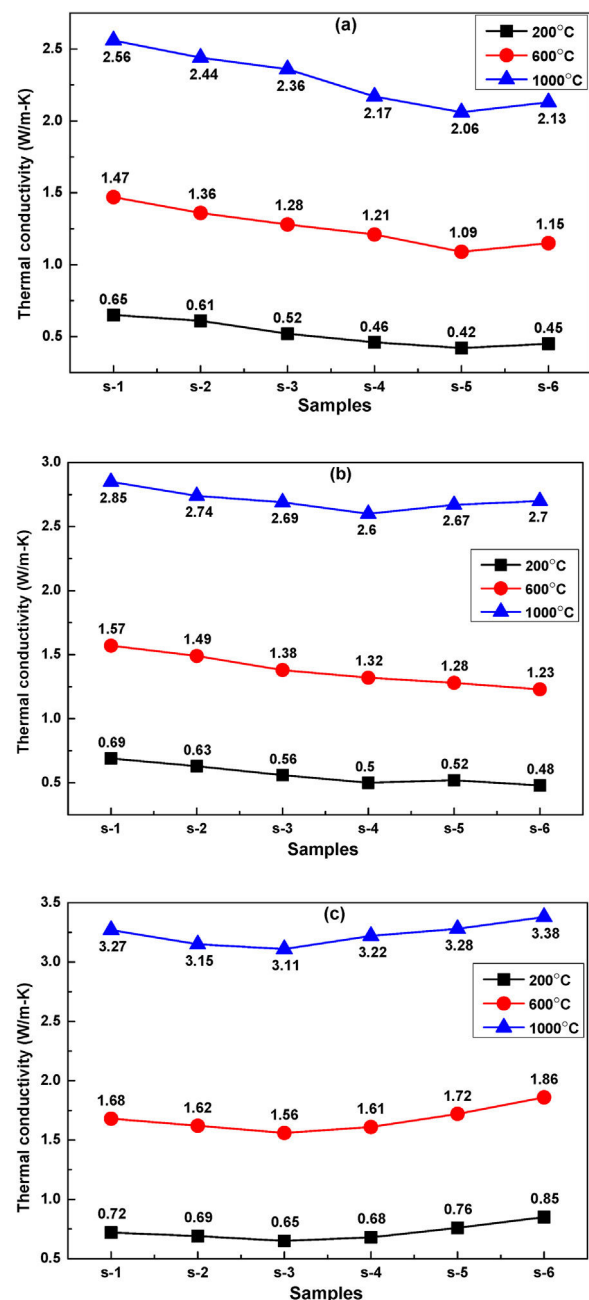

Fig. 10 – Temperature dependent thermal conductivity of different samples fired at (a) 800 °C, (b) 900 °C and (c) 1000 °C.
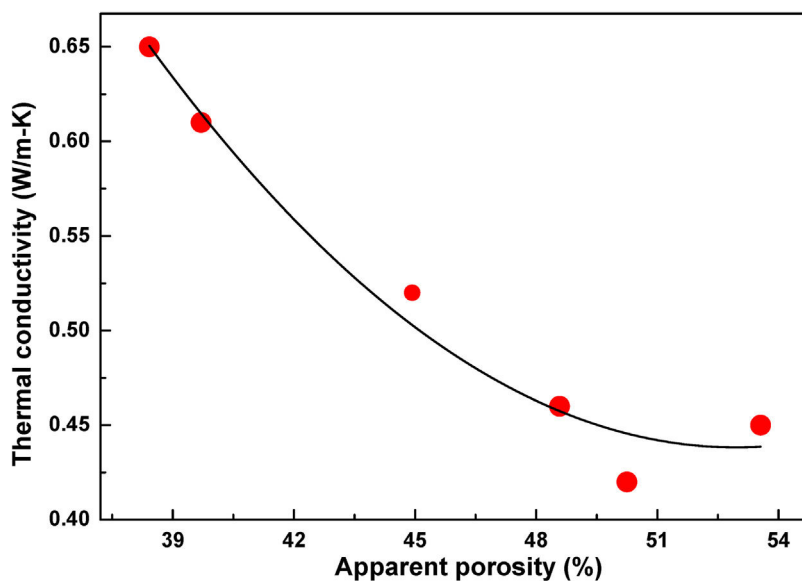
Fig. 11 – Relation between thermal conductivity and apparent porosity.

their contribution depends on the temperature mainly. At low temperatures (<300 °C) energy flow in materials mainly occurs via lattice vibrations (phonons) at speed of sound and significantly decreased to a lower value at higher temperatures, where the photon conductivity (radiation) mainly governed the conductivity. Generally, photon conductivity (radiation) increased with increasing temperature in crystalline materials, which is the principal mechanism of energy travel at high temperature through the materials [51]. This mood is a fast sequence of absorptions and emissions, of photons that transfer at the speed of light. This type of conduction is exclusively vital in porous ceramics like above refractory. As a result thermal conductivity of s-1 samples fired at 800 °C is 0.65 W/m K for 200 °C and 2.56 W/m K for 1000 °C.

Conclusions

It is established that substantial amounts of waste materials can be used to fabricate insulation refractory. The properties of insulation samples incorporating fly ash, rice husk ash, rice husk and fired refractory grog are investigated. Use of different wastes as a raw material in fabrication of insulation refractories can be a significant way of recycling for final disposal of these abundant wastes. Varying the FA content in mixtures it is possible to improve the insulation properties of sintered bodies. Results show excellent low thermal conductivity, high porosity, low density, good electrical resistivity, moderate CCS and flexural strength. Sample s-6 fired at 800 °C can be envisaged as a refractory material to be used for insulation purpose. The obtained results show that it would be promising for the large-scale synthesis of insulation bricks.

Acknowledgements

REFERENCES

[1] K. Katsube, M. Hashida, T. Tenra, Development of high-performance vacuum insulation panel, Matsushita Tech. J. 52 (6) (2006) 482–485.

[2] M. Sutcu, S. Akkurt, The use of recycled paper processing residues in making porous brick with reduced thermal conductivity, Ceram. Int. 35 (2009) 2625–2631.

[3] S. Dasgupta, S.K. Das, Paper pulp waste – a new source of raw material for the synthesis of a porous ceramic composite, Bull. Mater. Sci. 25 (2002) 381–385.

[4] R.H. Geraldo, L.F.R. Fernandes, G. Camarini, Water treatment sludge and rice husk ash to sustainable geopolymer production, J. Clean. Prod. 149 (2017) 146–155.

[5] L.C.S. Herek, C.E. Hori, M.H.M. Reis, N.D. Mora, C.R.G. Tavares, R. Bergamasco, Characterization of ceramic bricks incorporated with textile laundry sludge, Ceram. Int. 38 (2012) 951–959.

[6] H.B. Wang, Z.Z. Lin, Z.Y. He, A new brick prepared from municipal sewage sludge and shale, Adv. Mater. Res. 374–377 (2012) 18–23.

[7] M.H. Rahmana, M.T. Islama, T. Minhaja, M.A.K. Azada, M.M. Hasana, A.A.M.R. Haquea, Study of thermal conductivity and mechanical property of insulating firebrick produced by local clay and petroleum coal dust as raw materials, Proc. Eng. 105 (2015) 121–128.

[8] Y. Yin, B. Ma, S. Li, B. Zhang, J. Yu, Z. Zhang, G. Li, Synthesis of Al$_2$O$_3$–SiC composite powders from coal ash in NaCl–KCl molten salts medium, Ceram. Int. 42 (2016) 19225–19230.

[9] A.D. Onojah, N.A. Agbendeh, C. Mbakaan, Rice husk ash refractory: the temperature dependent crystalline phase aspects, IJRRAS 15 (2) (2013) 246–248.

[10] Y.C. Khoo, I. Johari, Z.A. Ahmad, Influence of rice husk ash on the engineering properties of fired clay brick, Adv. Mater. Res. 795 (2013) 14–18.

[11] B.S.D. Fonseca, A. Vilão, C. Galhano, J.A.R. Simão, Reusing coffee waste in manufacture of ceramics for construction, Adv. Appl. Ceram. 113 (3) (2014) 159–166.

[12] D. Eliche-Quesada, L. Pérez-Villarejo, F.J. Iglesias-Godino, C. Martínez-García, F.A. Corpas-Iglesias, Incorporation of coffee grounds into clay brick production, Adv. Appl. Ceram. 110 (4) (2011) 225–232.

[13] C. Bories, L. Aouba, E. Vedrenne, G. Vilarem, Fired clay bricks using agricultural biomass wastes: study and characterization, Constr. Build. Mater. 91 (2015) 158–163.

[14] A.A. Kadir, N.A.M. Zahari, N.A. Mardi, Utilization of palm oil waste into fired clay brick, Adv. Environ. Biol. 7 (12) (2013) 3826–3834.

[15] L. Aouba, M. Countand, B. Perrin, H. Lemercier, Predicting thermal performance of fired clay bricks lightened by adding organic matter: improvement of brick geometry, Build. Phys. 38 (6) (2015) 531–547.

[16] R.S. Blissett, N.A. Rowson, A review of the multi-component utilization of coal fly ash, Fuel 97 (2012) 1–23.

[17] Report on Fly Ash Generation at Coal/Lignite Based Thermal Power Stations and its Utilization in the Country for the Year 2016–17, Central Electricity Authority, Delhi, 2017 (http://www.cea.nic.in/reports/others/thermal/tcd/flyash_201617.pdf).

[18] F. Fan, Z. Liu, G. Xu, H. Peng, C.S. Cai, Mechanical and thermal properties of fly ash based geopolymers, Constr. Building Mater. 160 (2018) 66–81.

[19] G. Mucsi, Á. Szenczi, S. Nagy, Fiber reinforced geopolymer from synergetic utilization of fly ash and waste tire, J. Clean. Prod. 178 (2018) 429–440.

[20] M. Zhu, Z. Ru Ji, H. Li, L.L. Wang, L. Liu, Z. Zhang, Preparation of glass ceramic foams for thermal insulation applications from coal fly ash and waste glass, Constr. Building Mater. 112 (2016) 398–405.

[21] P. Hlaváček, V. Šmilauer, F. Škvára, et al., Inorganic foams made from alkali activated fly ash: mechanical, chemical and physical properties, J. Eur. Ceram. Soc. 35 (2) (2015) 703–709.

[22] T. Fukasawa, A. Horigome, A.D. Karisma, N. Maeda, A.N. Huang, K. Fukui, Utilization of incineration fly ash from biomass power plants for zeolite synthesis from coal fly ash by microwave hydrothermal treatment, Adv. Powder Technol. 29 (3) (2018) 450–456.

[23] Y. Luo, S. Zheng, S. Ma, C. Liu, J. Ding, X. Wang, Novel two-step process for synthesising β-SiC whiskers from coal fly ash and water glass, Ceram. Int. (2018) (https://doi.org/10.1016/j.ceramint.2018.03.082).

[24] A. Kumar, K. Sanjay, Development of paving blocks from synergetic use of red mud and fly ash using geopolymerization, Constr. Build. Mater. 38 (2013) 865–871.

[25] Y. Luo, S. Zheng, S. Ma, C. Liua, X. Wang, Ceramic tiles derived from coal fly ash: preparation and mechanical characterization, Ceram. Int. 43 (2017) 11953–11966.

[26] G. Han, S. Yang, W. Peng, Y. Huang, H. Wu, W. Chai, J. Liu, Enhanced recycling and utilization of mullite from coal fly ash with a flotation and metallurgy process, J. Clean. Prod. 178 (2018) 804–813.

[27] R. Pode, Potential applications of rice husk ash waste from rice husk biomass power plant, Renew. Sustain. Energy Rev. 53 (2016) 1468–1485.

[28] J.C.C. Cunha, E.M. Canepa, Aproveitamento energe'tico da casca de arroz, in: JPrograma energia, Research Project Report, Fundatec, Porto, Alegre, RS, 1986.

[29] A.K. Matori, M.M. Haslinawati, Producing amorphous white silica from rice husk, MASAUM J. Basic Appl. Sci. 1 (3) (2009) 512–515.

[30] M. Sarangi, S. Bhattacharyya, R.C. Behera, Effect of temperature on morphology and phase transformations of

nano crystalline silica obtained from rice husk, Phase Transit. 82 (5) (2009) 377–386.

[31] A. Bazargan, T. Gebreegziabher, C.W. Hui, G. McKay, The effect of alkali treatment on rice husk moisture content and drying kinetics, Biomass Bioenergy 70 (2014) 468–475 (https://doi.org/10.1016/j.biombioe.2014.08.018).

[32] M.R.F. Gonzalves, C.P. Bergmann, Thermal insulators made with rice husk ashes: production and correlation between properties and microstructure, Constr. Build. Mater. 21 (12) (2007) 2059–2065.

[33] F. Bondioli, L. Barbieri, A.M. Ferrari, T. Manfredini, Characterization of rice husk ash and its recycling as quartz substitute for the production of ceramic glazes, J. Am. Ceram. Soc. 93 (1) (2010) 121–126.

[34] S. Sembiring, Synthesis and characterisation of rice husk silica based borosilicate (B2SiO) ceramic by sol gel routes, Indones. J. Chem. 11 (1) (2011) 85–89.

[35] W. Simanjuntak, S. Sembiring, The use of the Rietveld method to study the phase composition of cordierite (Mg2Al4Si5O) ceramics prepared from rice husk silica, Makara J. Sci. 15 (1) (2011) 97–100.

[36] S. Sembiring, W. Simanjuntak, P. Manurung, D. Asmi, I.M. Low, Synthesis and characterisation of gel-derived mullite precursors from rice husk silica, Ceram. Int. 40 (5) (2014) 7067–7072.

[37] L. Mathur, S.S. Hossain, M.R. Majhi, P.K. Roy, Synthesis of nano-crystalline forsterite (Mg2SiO4) powder from biomass rice husk silica by solid-state route, Bol. Soc. Esp. Cerám. Vidr. 57 (2018) 112–118 (https://doi.org/10.1016/j.bsecv.2017.10.004).

[38] S.K. Singh, B.C. Mohanty, S. Basu, Synthesis of SiC from rice husk in a plasma reactor, Bull. Mater. Sci. 25 (6) (2002) 561–563.

[39] A. Bhardwaj, S.S. Hossain, M.R. Majhi, Preparation and characterization of clay bonded high strength silica refractory by utilizing agriculture waste, Bol. Soc. Esp. Cerám. Vidr. 56 (2017) 256–262.

[40] ASTM C356-10, Standard Test Method for Linear Shrinkage of Preformed High-Temperature Thermal Insulation Subjected to Soaking Heat, ASTM International, 2010.

[41] ASTM C133, Standard Test Methods for Cold Crushing Strength and Modulus of Rupture of Refractories, ASTM International, 2015.

[42] G. Görhan, O. Simsek, Porous clay bricks manufactured with rice husks, Constr. Build. Mater. 40 (2013) 390–396.

[43] J.G. Otero, F. Blanco, M.P. Garcia, J. Ayala, Manufacture of refractory insulating bricks using fly ash and clay, Br. Ceram. Trans. 103 (4) (2004) 181–186.

[44] A.R. Studart, T. Gonzenbach, E. Tervoort, L.J. Gauckler, Processing routes to macroporous ceramics: a review, J. Am. Ceram. Soc. 89 (2006) 1771–1789.

[45] Z. Li, Z. Luo, X. Li, T. Liu, L. Guan, T. Wu, A. Lu, Preparation and characterization of glass–ceramic foams with waste quartz sand and coal gangue in different proportions, J. Porous Mater. 23 (2016) 231–238.

[46] D.H. Vu, K.S. Wang, B.H. Bac, Humidity control porous ceramics prepared from waste and porous materials, Mater. Lett. 65 (2011) 940–943.

[47] S.M.S. Kazmi, S. Abbas, M.A. Saleem, M.J. Munir, A. Khitab, Manufacturing of sustainable clay bricks: utilization of waste sugarcane bagasse and rice husk ashes, Constr. Build. Mater. 120 (2016) 29–41.

[48] M. Sutcu, H. Alptekin, E. Erdogmus, Y. Er, O. Gencel, Characteristics of fired clay bricks with waste marble powder addition as building materials, Constr. Build. Mater. 82 (2015) 1–8.

[49] L. Aouba, C. Bories, M. Coutand, B. Perrin, H. Lemercier, Properties of fired clay bricks with incorporated biomasses:

cases of olive stone flour and wheat straw residues, Constr. Build. Mater. 102 (2016) 7–13.

[50] S.R. Bragança, A. Zimmer, C.P. Bergmann, Use of mineral coal ashes In insulating refractory brick, Refract. Ind. Ceram. 49 (4) (2008) 320–323.

[51] A.R. Pal, S. Bharati, N.V.S. Krishna, G.C. Das, P.G. Pal, The effect of sintering behaviour and phase transformations on strength and thermal conductivity of disposable tundish linings with varying compositions, Ceram. Int. 38 (2012) 3383–3389.